The effect of pre-processing and grain structure on the bio-corrosion and fatigue resistance of magnesium alloy AZ31

H. Wang [a,*], Y. Estrin [b], H. M. Fu [c], G.L. Song [c#] and Z. Zúberová [d]

[a] Faculty of Engineering & Surveying, University of Southern Queensland, Toowoomba, Queensland 4350, Australia

[b] ARC Centre of Excellence for Design in Light Metals, Department of Materials Engineering, Monash University, Clayton, VIC 3800, Australia and CSIRO Division of Manufacturing and Materials Technology, Clayton, Vic. 3168, Australia

[c] School of Engineering, The University of Queensland, St Lucia 4072, Australia

[d] Department of Material Science and Engineering, Clausthal University of Technology, 38670 Clausthal-Zellerfeld, Germany

[#] Current corresponding address: GM R&D Center, MC: 480-106-212; 30500 Mound Rd., Warren, MI48090-9055, USA.

Magnesium alloys are broadly used for structural applications in the aerospace and automotive industries as well as in consumer electronics. While a high specific strength is the forte of magnesium alloys, one serious limitation for Mg alloys is their corrosion performance. Unlike aluminium, it does not form a stable passive film to provide long-term protection from further corrosion. The poor corrosion resistance of magnesium and magnesium alloys is regarded as a major drawback, and significant effort has been focused on improving this.[1-3] However, the high reactivity of magnesium alloys in corrosive media can be used to advantage in biomedical applications, particularly in temporary implants where the capacity of a material for bio-degradation is one of the most sought after properties. Indeed, permanent implant materials, such as stainless steel, titanium alloys or Nitinol (55Ni-45Ti), are the only choices currently available for hard tissue implantation. They can cause permanent physical irritation, long-term endothelial dysfunction and chronic inflammatory local reaction. Sometimes a second operation is needed for the implant to be removed. Given the ability of the human body to gradually recover and regenerate damaged tissue, the ideal solution would thus be a degradable implant, which would offer a physiologically less invasive repair and temporary support during tissue recovery. After fulfilling its function, this implant would be obliterated, being absorbed by the body. This philosophy of implant surgery would also be of particular interest for endovascular stents.

A high propensity for corrosion makes magnesium alloys potential candidates for biodegradable implant materials. In fact, magnesium is actually present in large amounts in the human body and it is involved in many metabolic reactions and physiological mechanisms. The recommended daily intake for magnesium is 300-400 mg/day. In bone implants, magnesium is also one of the most important bivalent ions in the formation of biological apatites. In addition to magnesium being biocompatible and essential to human metabolism, it has further advantages over other implant materials. These are as follows: (i) the density of Mg (1.74 g/cm^3) is similar to that of natural bone (1.75 g/cm^3), (ii) with alloying, high strength levels, up to 330 MPa, can be achieved, and (iii) its Young's modulus, E, (45 GPa) is also similar to that of natural bone (40-57 GPa), as opposed to that of titanium alloys (whose E-values are too high) and organic synthetic materials (where E is too low).

The potential of magnesium alloys as biodegradable implant materials has been recognised by several authors, and notable research activities in this field are underway.[4-7] For magnesium and its alloys to be usable as biodegradable implant materials, first their

degradation rates should be consistent with the rate of healing of the affected tissue, and the degradation products should be within the body's acceptable absorption levels; secondly, the material should have a good fatigue resistance, as an implant is commonly exposed to a large number of loading and unloading cycles. As an example, an endovascular stent is subjected to tens of millions of cycles during service.[8] These properties can be adjusted in various ways, particularly by alloying and impurity control and thermomechanical treatment. In this paper we report our results on the fatigue and bio-corrosion resistance of AZ31, which is one of the most common magnesium alloys used for structural applications.

Experimental

Materials Preparation

Magnesium alloy AZ31 was used as test material. While the Zn content corresponded to the nominal one (1 wt %), the actual Al content was 3.76 wt %, i.e. higher than the nominal 3 wt%. Generally, magnesium alloys exhibit better mechanical properties than pure magnesium. Mg-Al-Zn alloys (the AZ series) are the most widely used magnesium alloys because of their superior mechanical properties and good castability. Small amounts of aluminium, zinc and manganese contained in the alloy do not show excessive cell toxicity as these elements are also naturally present within the human body. However, higher levels of aluminium in the alloy (that may be desirable from the enhanced strength viewpoint) will have an adverse effect on biocompatibility. The possibility of using of AZ31 as biodegradable material has also been considered by others.[4]

The material used in this study was produced by charging raw materials in an electric resistance furnace. Three material states were investigated. Squeeze cast (SC) material was fabricated in a two-step squeeze casting process with initial squeeze pressure of 80 MPa applied for 15 seconds, followed by 140 MPa pressure applied for 90 seconds. The casting temperature was approximately 720°C and the die temperature approximately 200°C. Hot rolled (HR) material was obtained by rolling the SC material at 370 °C to a thickness reduction of 75%. Finally, a third material state was obtained by further processing the HR material by equal channel angular pressing (ECAP). In this processing step, square shaped 10 mm x 10 mm x 100 mm billets were subjected to 4 passes of ECAP through a 90° die at a ram speed of 5 mm/min. After each ECAP pass, the specimen was rotated by 90° in the same sense (ECAP Route B_c). The ECAP die temperature was 200°C.

Degradation test

SC, HR and ECAP samples were cut to a thickness in the range of 2-2.5 mm. The edges of the specimens were ground. The specimens were then polished finishing with 4000 grid SiC paper and degreased with ethanol. Degradation tests were conducted by immersing the specimens in a Hank's balanced salt solution with a composition: $CaCl_2$ 0.14 g/l, KCl 0.4 g/l, NaCl 8.0g/l, $MgSO_4$ 0.1 g/l, KH_2PO_4 0.06 g/l, $NaHPO_4$ 0.05 g/l and D-Glucose 1.0 g/l. The immersion test was used to simulate the biochemical reaction of the magnesium alloys in human physiological conditions. The specimens were suspended in Hank's solution for 1, 2, 5, 10, 15 and 20 days. The pH of the solution was monitored by a portable pH meter and adjusted at a value of 7 by using 1N HCl and 1N NaOH. After the specified immersion time, the specimens were observed in an optical microscope to record the surface appearance. The specimens were then washed with a solution containing CrO_3 and $AgNO_3$ to remove the corrosion products and weighed. Two samples were used for each immersion time and the average of the weight loss results was taken.

The electrochemical impedance spectra (EIS) of the alloy in the SC condition were also measured in the same Hank's solution at their corrosion potentials using a Solatron 1287 + 1255B electrochemical measurement system. The amplitude of AC signal was 5 mV. The frequency range was set from 7 kHz to 10 mHz, but EIS measurements were stopped before the low frequency limit was reached, as data in the in the low frequency region showed large scatter.

Fatigue tests

Cylindrical specimens with diameter of either 5 or 8 mm were used for fatigue testing in a servohydraulic Instron 8501 testing machine. Symmetrical tension-compression loading was carried out at room temperature (air) under load control with a frequency of 20 Hz. At least three specimens were tested for each stress amplitude.

Optical microscopy and transmission electron microscopy (TEM) were used for microstructure characterisation. To that end, light microscopy specimens of the coarse-grained SC material were cut from castings, in no specific direction and without casting skin. Specimens prepared from HR material had their longitudinal direction aligned with the rolling direction. Finally, TEM specimens of ECAP material were extracted from the middle part of the billets, the TEM foil plane being perpendicular to the pressing direction. The foils were mechanically polished and electropolished at – 45°C in a Tenupol 5 double jet polishing unit in a LiCl + Mg perchlorate + methanol + buthyloxyethanol solution. TEM micrographs were obtained using a Philips CM 200 electron microscope.

Results and discussion

Microstructure

Light microscopy samples of SC material were cut at random from the cast billets. Figure 1 shows a typical coarse-grained dendritic structure with average grain size of about 450 μm observed. Grain size was measured using the linear intercept method outlined in section E112-88 of ASTM Standard, 1994.

The microstructure of the HR material is presented in Figure 2. It is seen that hot rolling changes the microstructure of the as-cast material significantly, in terms of both the size and the morphology of the grains. The dendritic structure has totally disappeared as a result of hot rolling. The material now possesses a uniform and fine equiaxed microstructure with the average grain size of about 20 μm.

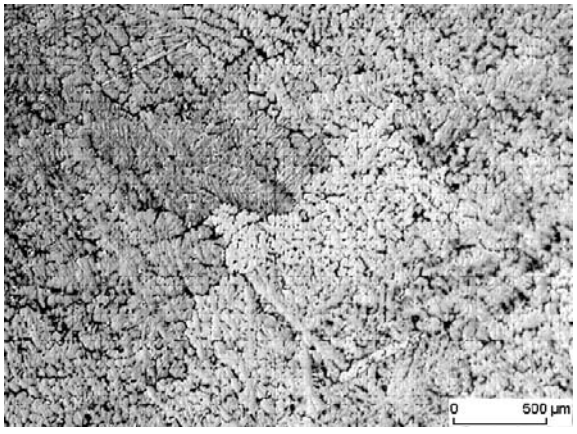

Fig. 1 Typical microstructure of the SC material.

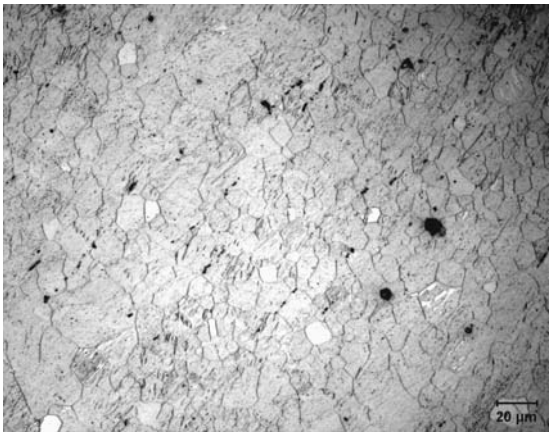

Fig. 2 Typical microstructure of the HR material.

The ECAP processed material exhibits an even finer grain structure than the HR one. The homogeneous microstructure of the ECAP material with a grain size of about 2.5 μm is shown in Figure 3. A TEM image of the characteristic grain structure produced by severe plastic deformation by ECAP is presented Figure 4.[9]

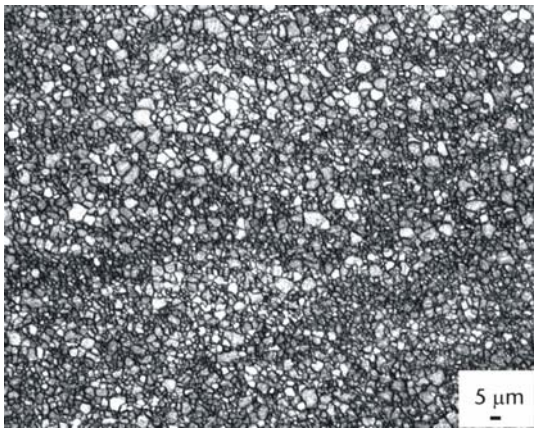

Fig. 3. Typical microstructure of ECAP samples after 4 ECAP passes.

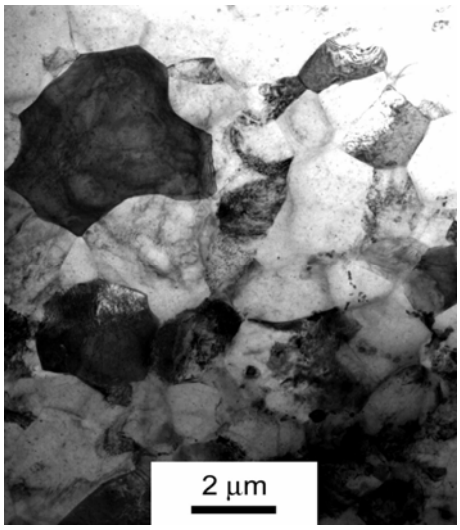

Fig. 4. Representative microstructure of ECAP processed material (4 ECAP passes), after Ref. 9.

Fatigue behaviour

The fatigue results for the three material states investigated here are reported in Ref. 9. They are summarised in Figure 5 showing the respective S-N curves. Additional data points for the ECAP processed material are also included. The maximum number of cycles to which the tests were run was 10^7. The horizontal arrows refer to the data points in which no failure occurred within 10^7 cycles. It can be seen that the manufacturing procedures leading to the three different states of the material and the concomitant grain structures have a strong effect on the fatigue properties. The SC material exhibits the lowest fatigue strength, the endurance limit (taken as the stress amplitude at 10^7 cycles) being about 40 MPa. Hot rolling is seen to improve the fatigue strength of the SC material. Indeed, the endurance limit of the HR material (95 MPa) is more than twice as high as that of the SC one. Interestingly enough, ECAP processing of the HR material, while further reducing the grain size, does not enhance the endurance limit. The fatigue life of the ECAP material is somewhat lower than that of the HR material, the data points for the former being shifted towards lower numbers of cycles. In an earlier publication[9] it was shown that both the HR and the ECAP material show a combination of mechanical properties superior to those of the SC material. This refers, in addition to the endurance limit, to both the fatigue life and the ultimate tensile strength. However, no clear relation between these properties and the grain size could be established. It was conjectured[9] that strengthening due to grain refinement may be counterbalanced by a reduction in strength associated with texture softening, see also.[10]

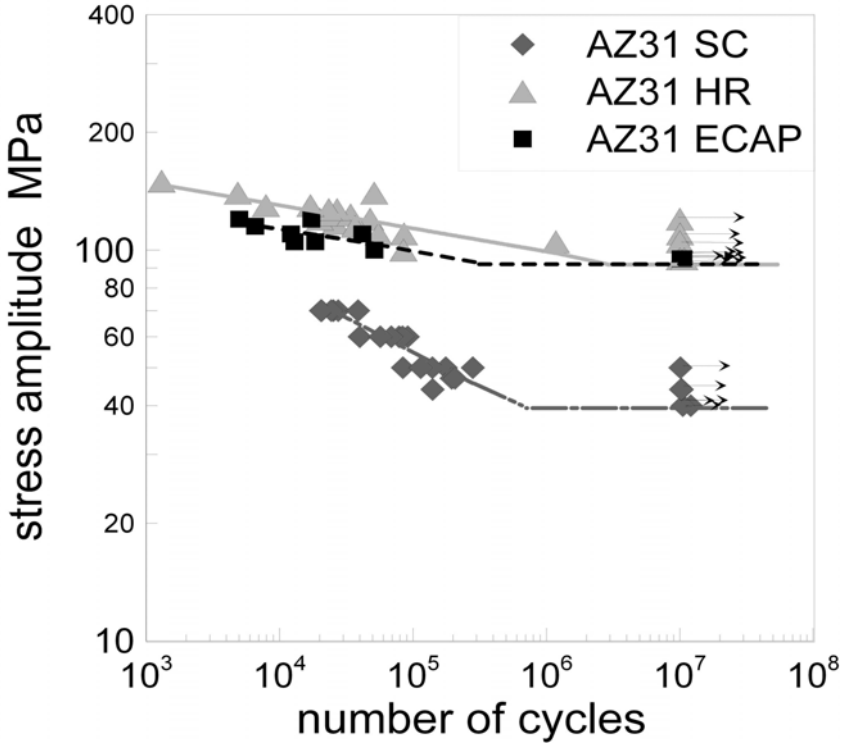

Fig. 5 Fatigue properties for the three states of the material.

Degradation behaviour

The degradation behaviour of the SC, HR and ECAP samples was investigated in immersion tests under simulated physiological conditions. The weight loss after a preset number of days of immersion was measured for all three materials. The degradation rate was calculated as grams per exposure-area per time, and was converted to thickness loss rate of a constant area sample, in micrometer per day. The results are plotted in Figure 6. The degradation process, starting off with a high degradation rate, is seen to slow down with the immersion time. The retardation of the degradation process with time stems from the accumulation of the corrosion products on the specimen surface. Beside the main corrosion products, magnesium hydroxide as well as other phosphates and carbonates were produced. They formed a layer on the surface of the sample, retarding the corrosion process. It should be stressed that the alloying elements Al and Zn in the alloy tend to have a beneficial effect on the stability of the protective film formed. Indeed, pure magnesium without these alloying elements experiences a much faster biodegradation under similar testing conditions.[11] It was found[15] that in Hank's solution the rate of hydrogen evolution that reflects the biodegradation rate increases with time for pure magnesium, while for a magnesium alloy containing Al or Zn the biodegradation rate decreases with time. Thus

the degradation behaviour of alloy AZ31 reported in this paper is in agreement with other studies[15] on biodegradation of magnesium alloys in a similar simulated body fluid.

While the degradation behaviour for all three material conditions (SC, HR, and ECAP) shows a similar qualitative trend, with the corrosion rate decreasing with the immersion time, significant quantitative differences in their degradation kinetics are obvious. SC samples exhibited a much higher degradation rate than the material in the other two conditions. The initial degradation rate for the SC samples was 2.08 μm/day or 0.35 mg/day/cm^2; after 20 days of immersion (the longest test duration) it decreased to 0.87 μm/day or 0.15 mg/day/cm^2. The degradation rates of the HR and ECAP samples were initially different (1.33 and 1.49 μm/day, respectively), but after the first two days practically no difference in the degradation rate was observed. At the end of the 20 days testing, the degradation rate of both materials was about 0.74 μm/day. The reduced corrosion rate of AZ31 by HR treatment must be associated with the grain refinement effect. A further reduction of the grain size by ECAP did not lead to a decrease in the corrosion rate. The reasons for that, and the possible role of the dislocations and vacancies produced by ECAP, are yet to be investigated.

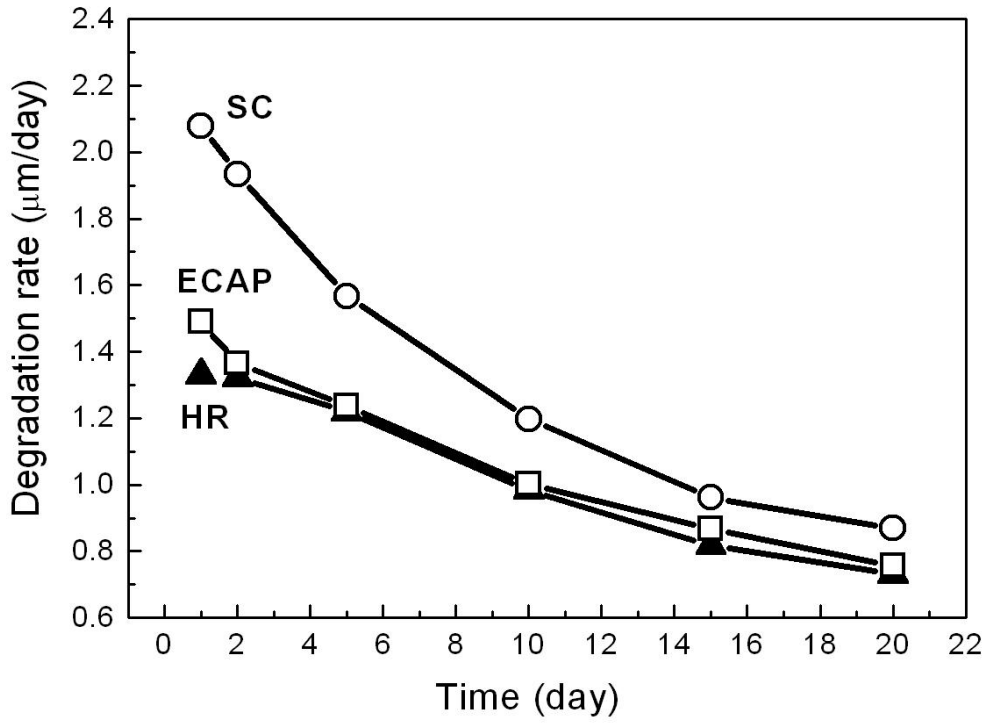

Fig. 6. Degradation rate of SC, HR and ECAP samples in Hank's solution under static conditions.

Figure 7 shows the surface morphology of the SC, HR and ECAP samples after immersion testing. From the appearance of the immersed samples, it was determined that the corrosion damage in static solution was mainly localised pitting. Pitting can expand with the immersion time, as shown by the arrows in Figure 7. In fact, magnesium alloys normally suffer from non-uniform corrosion attack.[1] Many factors can cause pitting corrosion damage of magnesium alloys, such as the non-uniformly formed corrosion product film, the micro-galvanic effect of impurity particles and secondary phases within the matrix phase as well as non-uniformity of

alloy composition. Previous studies[12] showed that under dynamic conditions, the protective film was not stable, and uniform corrosion at a much higher rate was observed for high solution flow rates. Obviously, a flowing medium can reduce the effect of some of the above factors on the corrosion process.

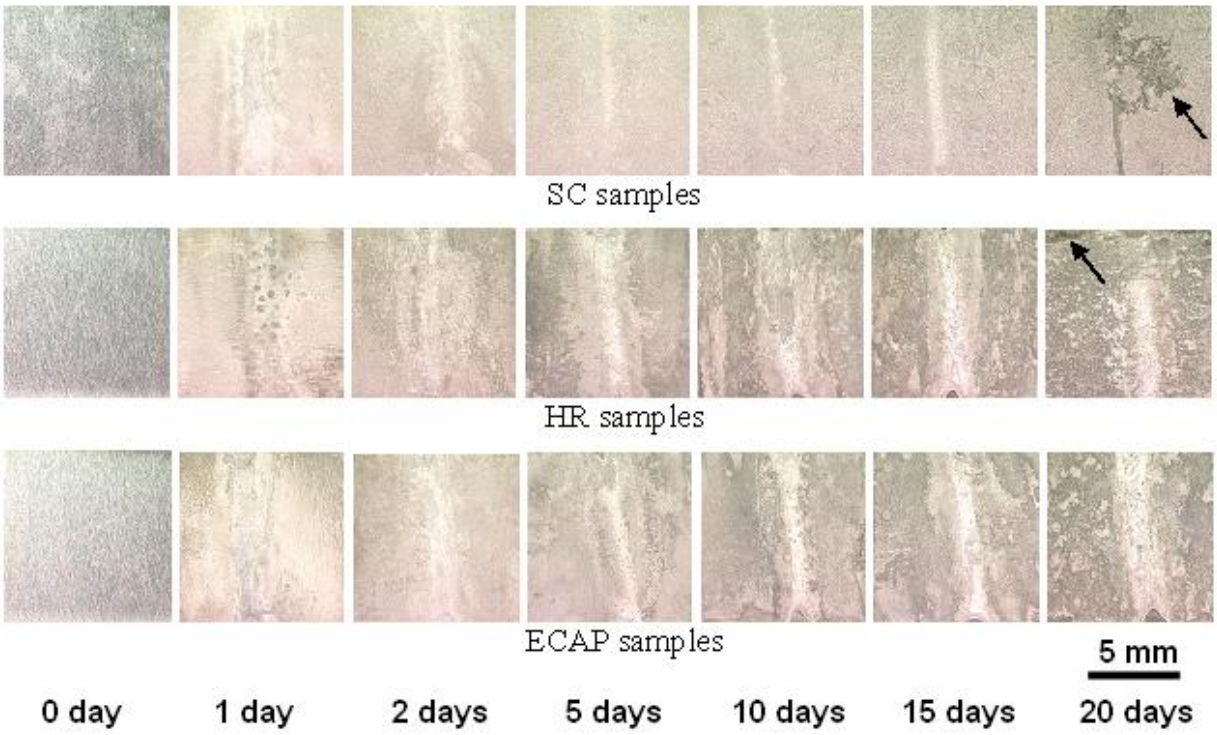

Fig. 7. Surface appearance of SC, HR and ECAP samples that have been immersed in Hank's solution for up to 20 days. Regions of severe attack after 20 days are arrowed.

Electrochemical behaviour

Electrochemical impedance spectra (EIS) of AZ31 were used to monitor the variation of corrosion rate in the early stage, which may provides some information on the formation of the corrosion products during the degradation process. These measurements were only carried out for the alloy in the SC condition. The measurement data are represented in a diagram in which the imaginary part of the impedance Z is plotted against its real part. Such diagrams usually exhibit several semi-circles corresponding to distinct individual processes in the electrode system. However, the data points in the low frequency region showed too much scatter to signify the corrosion reaction mechanism, so they are not included . Nethertheless, the lack of the low frequency spectra does not affect the following discussion in this paper, as the low frequency EIS features are insignificant compared with the capacitive loop in the high frequency region[11]. Neglecting the low frequency spectra would not introduce significant error in the estimation of the corrosion rate in this study. A typical AC EIS for SC specimens immersed in Hank's solution for various times is shown in Figure 8. There is clearly a semi-circle (albeit somewhat deformed and not fully symmetric) found in each EIS measurement, as illustrated in Figure 8. This indicates that there is at least a simple electrochemical process dominated by the mechanism of charge transfer across the interface between AZ31 and the

solution involved in the degradation of AZ31 in Hank's solution. Although the size of the near semi-circular curve increased with time, the basic process remained unchanged for the duration of the test, suggesting that the degradation mechanism of AZ31 in Hank's solution did not change despite the rate variation of the charge transfer during the degradation process.

The polarization resistance of the samples immersed in the solution can be obtained from the diameters of the near semi-circular spectra. The results are plotted in Figure 9 as a function of the immersion time. Since the resistance can be related to the corrosion rate through the Geary-Stern equation,[13] the changes of the measured spectra with the immersion time to some extent represent the initial corrosion behaviour of AZ31 in the Hank solution. It is seen clearly that in the first 20 hours, the corrosion resistance continuously increases with time. This is consistent with the decreasing tendency of the corrosion rate with time observed in Figure 6. The increase of polarisation resistance with time suggests that a protective film may have formed and kept growing on the surface of the specimens while they were immersed in the solution. It can be conjectured that the film formed on the AZ31 alloy in Hank's solution consists of corrosion products having a protective effect, the thickening of the film thus contributing to an increase in polarisation resistance. Unlike a passive film, though, it cannot completely stop the corrosion attack caused by chloride ions. Thus, after long term exposure to the corrosive Hank solution, the specimens were still corroding in some areas. XPS analysis of a sample that had been immersed in Hank's solution identified the main constituents of the layer deposited as a result of a reaction between AZ31 and the solution as $Mg_3(PO_4)_2$, $Ca_3(PO_4)_2$, $Mg(OH)_2$ and some $CaCO_3$.[14] A mixture of these corrosion products may provide resistance against further corrosion, which is reflected in a decrease in the degradation rate with time seen in Figure 6. Further investigations are needed to identify the detailed mechanisms underlying this behaviour and to understand the reasons for the quantitative differences in the corrosion kinetics of the SC and the mechanically processed specimens.

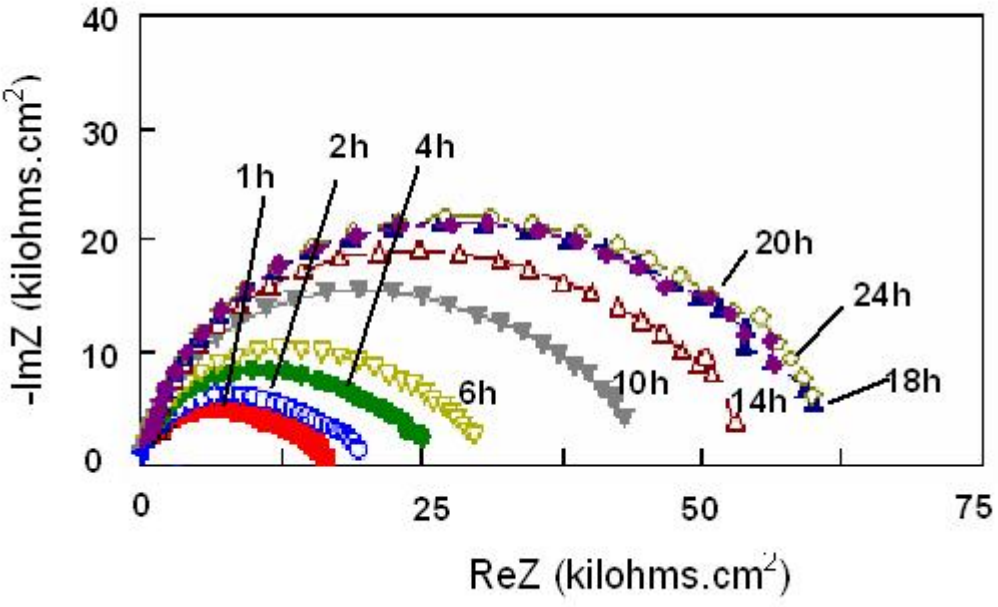

Fig. 8. EIS of SC AZ31 after immersion in Hank's solution for up to 24 hours.

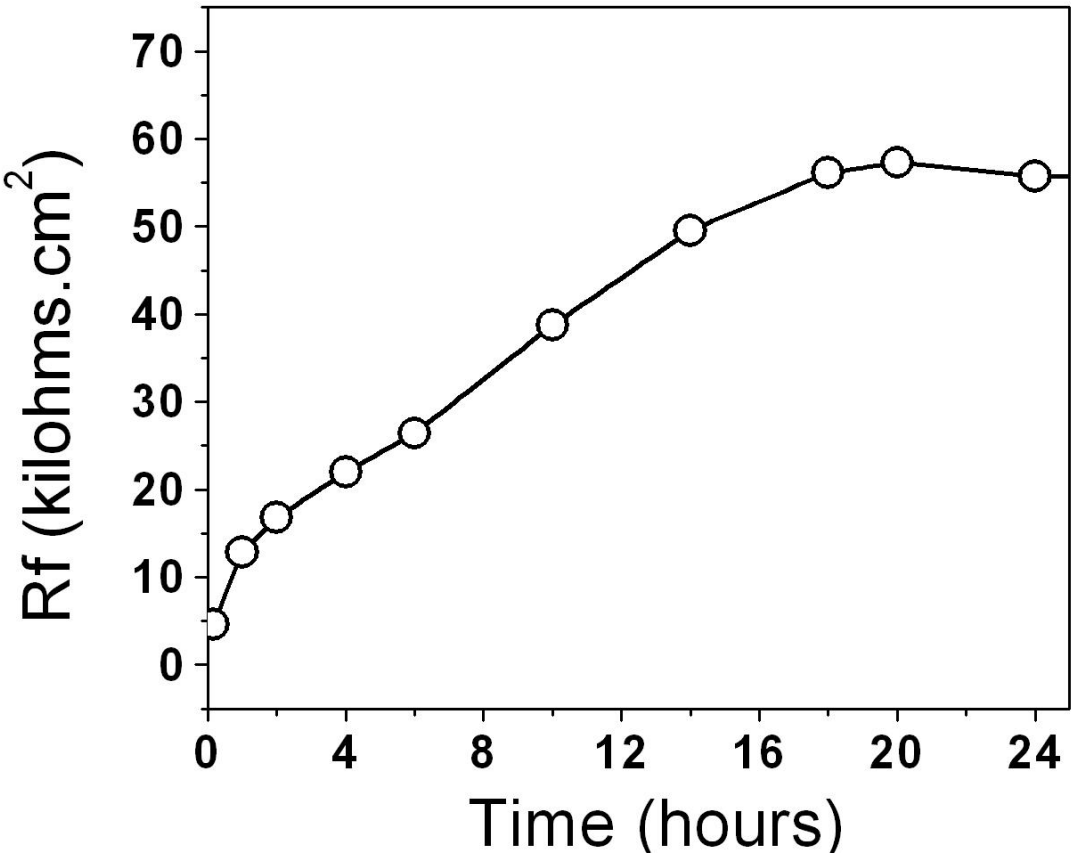

Fig. 9. Time dependence of the polarisation resistance of SC AZ31 immersed in Hank's solution.

Conclusions

The present study has shown that the microstructural condition of alloy AZ31 (which can be influenced by mechanical processing) has a pronounced effect on both the fracture resistance and the corrosion resistance of the alloy in Hank's solution. These are the properties which are among the most important ones in selecting an implant material for surgical applications.

Grain refinement by hot rolling has been shown to lead to a significant enhancement of fatigue life and endurance limit, as well as a reduction in corrosion rate. While fast corrosion kinetics is generally beneficial in biodegradable implants, the corrosion rate achieved with candidate magnesium alloys is too high for their use for surgical applications. Hot rolling and the concomitant grain refinement do provide a desirable retardation of corrosion. However, the anticipated further deceleration of corrosion in Hank's solution upon extreme grain refinement by subsequent ECAP processing of the HR material was not confirmed. Neither did ECAP increase the fatigue resistance. In contrast, it gave rise to a slight deterioration of both the fatigue and the corrosion resistance.

While a reduction of the endurance limit, which occurs despite a very significant further grain refinement due to ECAP processing, can be explained in terms of textural softening, we currently do not have an explanation for a slight acceleration of the degradation process caused by ECAP (which is more prominent at the beginning of the immersion test). It may be associated with a higher density of grain boundaries and a higher dislocation density resulting from severe plastic deformation. Interplay of these factors needs to be investigated in more detail.

The main conclusion from the current results is the possibility to significantly influence – and possibly to control – the fatigue behaviour and the corrosion rate in Hank's solution of a candidate implant material, magnesium alloy AZ31. An implication of this conclusion is that, in addition to the approaches recently proposed to enhance the biodegradability of magnesium, such as purification, alloying and anodising[15], mechanical processing could be a new way to make a magnesium alloy to a viable biomaterial.

Acknowledgements

The authors are thankful to Dr. Z.M. Shi for his assistance with the electrochemical measurements and to Prof. L. Kunz and Dr. M. Janecek for their contribution to the fatigue and TEM investigations. Helpful suggestions of Dr. R. O'Donnell and Dr. S. Furman are gratefully appreciated.

References

[1] G. Song, *Adv. Eng. Mater.* **2005**, 7, 563.

[2] J. E. Gray, B. Luan, *J. Alloys Comp.* **2002**, 336, 88.

[3] G. Song, A. Atrens, *Adv. Eng. Mater.* **1999**, 1, 11.

[4] F. Witte, V. Kaese, H. Haferkamp, E. Switzer, A. Meyer-Lindenberg, C. J. Wirth, H. Windhagen, *Biomater.* **2005**, 26, 3557.

[5] Y. B. Ren, J. J. Huang, K. Yang, B. C. Zhang, Z. M. Yao, H. Wang, *Acta Metall. Sinica.* **2005**, 41, 1228.

[6] A. Eliezer, F. Witte, *7th Intl. Conf. on Magnesium Alloys and Their Applications*, Wiley-VCH, Weinheim **2007**, 822.

[7] J. Levesque, D. Dube, M. Fiset, D. Mantovani, *Mater. Sci. Forum.* **2003**, 426-432, 521.

[8] S. W. Robertson, R. O. Ritchie, *Biomater.* **2007**, 28, 700.

[9] Z. Zúberová, L. Kunz, T. T. Lamark, Y. Estrin, M. Janeček, Metall. *Mater. Trans. A* **2007**, DOI: 10.1007/s11661-007-9109-6.

[10] S. R. Agnew, J. A. Horton, T. M. Lillo, D. W. Brown, *Scripta Mater.* **2004**, 50, 377.

[11] G. Song, S. Song, *Adv. Eng. Mater.* **2007**, 9, 298.

[12] H. Wang, M. X. Zhang, Z. M. Shi, K. Yang, *Tissue Eng.* **2006**, 12, 1067.

[13] M. Stern, A. L. Geary, *J. Electrochem Soc.* **1957**, 104, 56.

[14] H. Wang, M. X. Zhang, Z. M. Shi, K. Yang, *2006 TMS Conference*, San Antonio, USA, March 12-16, **2006**.

[15] G. Song, *Corrosion Science*, **2007**, 49, 1696